Characteristic mode based tradeoff analysis of antenna-chassis interactions for multiple antenna terminals

Li, Hui; Tan, Yi; Lau, Buon Kiong; Ying, Zhinong; He, Sailing

Published in:
IEEE Transactions on Antennas and Propagation

DOI:
10.1109/TAP.2011.2173438

2012

Document Version:
Peer reviewed version (aka post-print)

Characteristic Mode Based Tradeoff Analysis of Antenna-Chassis Interactions for Multiple Antenna Terminals

Hui Li, *Student Member, IEEE,* Yi Tan, Buon Kiong Lau, *Senior Member, IEEE,* Zhinong Ying, *Senior Member, IEEE,* and Sailing He, *Senior Member, IEEE*

***Abstract*—The design of multiple antennas in compact mobile terminals is a significant challenge, due to both practical and fundamental design tradeoffs. In this paper, fundamental antenna design tradeoffs of multiple antenna terminals are presented in the framework of characteristic mode analysis. In particular, interactions between the antenna elements and the characteristic modes and their impact on design tradeoffs are investigated in both theory and simulations. The results reveal that the characteristic modes play an important role in determining the optimal placement of antennas for low mutual coupling. Moreover, the ability of antenna elements to localize the excitation currents on the chassis can significantly influence the final performance. To demonstrate the effectiveness of the proposed approach, a dual-band, dual-antenna terminal is designed to provide an isolation of over 10 dB for the 900 MHz band without additional matching or decoupling structures. A tradeoff analysis of bandwidth, efficiency, effective diversity gain and capacity is performed over different antenna locations. Finally, three fabricated prototypes verify the simulation results for representative cases.**

***Index Terms*—Antenna array mutual coupling, MIMO systems, mobile communication**

I. Introduction

THE phenomenal success of multiple-input multiple-output (MIMO) technology can be seen in its critical role of enabling high data rates in Long Term Evolution (LTE), Worldwide Interoperability for Microwave Access (WiMAX) and IEEE802.11n. The key advantage of MIMO is its potential to linearly increase channel capacity with the number of antennas at both the transmitter and receiver, without sacrificing additional frequency spectrum and transmitted power [1]. However, implementing multiple antennas in compact terminal devices such as mobile phones is challenging, since it involves both practical and fundamental design tradeoffs [2]. Practical tradeoff considerations include the allocation of more antenna locations on the terminal and an increased likelihood of one or more antennas being detuned by the hand or head of the user. Nevertheless, most attention in the area has been on the fundamental aspect of closely spaced antennas resulting in an increase in spatial correlation and mutual coupling, which in turn degrade the performance of MIMO systems as measured by metrics such as efficiency, bandwidth, diversity gain and capacity [2]-[5].

Recent results indicate that, in a rich scattering environment, the MIMO performance of closely spaced antennas can be improved by decoupling multiple antennas, with the tradeoff being a smaller bandwidth [2], [5]. Decoupling techniques that are suitable for multiple antennas on small printed circuit boards (PCBs) are presented in [6]-[10]. Unfortunately, most of these techniques focus on the relatively high frequency bands, including the WLAN, DCS1800 and UMTS bands, and they have not been demonstrated for the mobile bands below 1 GHz, such as GSM900 and WCDMA850. To our understanding, there are several reasons for this. First, since the wavelength at 900 MHz is twice as long as that of 1800 MHz, for the same PCB, the available electrical distance between the antennas is only half of that at 1800 MHz. This complicates the isolation of the antennas. Second, some decoupling techniques, such as neutralization line [6] and quarter-wavelength slot filter [7], base their mechanisms on wavelength. If the frequency decreases, the dimensions of these decoupling structures will increase correspondingly, and they can take too much space on the PCBs. Even more importantly, the mobile chassis, which only functions as a ground plane for the antenna elements at high frequency band, becomes the main radiator at the low frequency bands [11]. Thus, different antenna elements share the same radiator, making isolation worse (e.g., the prototype in [12]). This aspect will be further explained in this paper.

The above discussion reveals that the influence of the mobile chassis becomes the most critical factor for multiple antenna terminals at the low frequency bands. However, nearly all existing studies of the impact of chassis on antenna design

Manuscript received June 1, 2010. This work was supported in part by VINNOVA under grant no. 2009-04047 and 2008-00970, and also in part by a scholarship within EU Erasmus Mundus External Cooperation Window Lot 14.

H. Li, Y. Tan and B. K. Lau are with the Department of Electrical and Information Technology, Lund University, SE-221 00 Lund, Sweden. E-mail: {Hui.Li, Yi.Tan, Buon_Kiong.Lau}@eit.lth.se. H. Li is also with school of Electromagnetic Engineering, Royal Institute of Technology, Sweden, and the Center for Optical and Electromagnetic Research, Zhejiang University, Hangzhou, 310058, China.

Z. Ying is with Research and Technology, Corporate Technology Office, Sony Ericsson Mobile Communications AB, SE-221 88 Lund, Sweden. E-mail: Ying.Zhinong@sonyericsson.com

S. He is with the Center for Optical and Electromagnetic Research, Zhejiang University, Hangzhou, 310058, China, and also with School of Electromagnetic Engineering, Royal Institute of Technology, SE-100 44 Stockholm, Sweden. E-mail: sailing@kth.se

focus their attention on single antenna design, e.g., [13]-[16]. In [13], a detailed study shows that self-resonant antenna elements can be replaced by smaller non-resonant antenna elements (or "coupling elements") that utilize the chassis as the radiating structure, thereby reducing the volume of the mobile terminal antenna. Mobile chassis can also be used to enhance the bandwidth of terminal antennas [14], [15] and create multiple resonances [16]. A recent simulation study [17] concludes that the impedance, bandwidth and radiation mode of an antenna on a ground plane is often defined by the location of the antenna and its feeding point, rather than the size of the ground plane.

While useful insights are provided by these studies, the results are based on the single antenna case, and hence may not be directly applicable to multiple antennas implemented on the same chassis. Some results for the multiple antenna case are presented in [18], where an oscillation of correlation coefficient is observed when two antennas with a fixed separation distance move along a large PCB with a length of 2.5λ. However, while the phenomenon is attributed to characteristic mode [19] (also called 'chassis mode' in [15], [16]), no further analysis is given.

To analyze the mobile chassis, different tools can be utilized, such as resonator based equivalent circuit [20], flat dipole equivalent circuit [21] and theory of characteristic mode [22]. Among these tools, a characteristic mode based analysis is an efficient way to gain physical insight into fundamental electromagnetic properties of mobile chassis and yield valuable information on antenna design. In particular, since characteristic modes are independent of excitation, and only depend on the shape of the chassis [23], the characteristic radiation properties can be obtained from mode analysis.

The purpose of this paper is to provide a framework in understanding fundamental design tradeoffs of multiple antennas on mobile chassis at low frequency bands through characteristic mode analysis and antenna simulations. The main contributions are:

- Using the theory of characteristic mode and supporting simulations to give insights into the mechanisms that govern the location dependent performance of multiple antennas on a mobile chassis.
- Relating the ability of a given type of antenna (i.e., monopoles and planar inverted F antennas (PIFAs)) to localize the excitation current on the chassis to the performance of multiple antennas.
- Achieving good MIMO performance, including isolation, efficiency and diversity gain, by taking advantage of the characteristics of antennas on the chassis, without the need for additional matching or decoupling structures.
- Providing tradeoff analyses for the performance of multiple antenna terminals with respect to the locations of the antenna elements, in terms of bandwidth, efficiency, correlation, diversity gain and capacity.

It should be emphasized that even though this paper focuses on the 900 MHz band, it is only intended to highlight the practicality of our proposal for typical mobile terminals sizes. The underlying principles are based on electrical dimensions rather than absolute dimensions, and hence more general. In other words, chassis radiation of existing or future mobile devices with different chassis sizes is significant in other frequency bands.

The paper is organized as follows: Section II briefly reviews the theory of characteristic mode and its application in providing fundamental characteristics of chassis radiation. The resonant characteristic electric fields, the eigenvectors and the modal significance (MS) [23] of a chassis are used to give helpful information on antenna design. A slot monopole on the chassis is also investigated using the characteristic mode analysis. Antenna simulations are carried out using an electromagnetic (EM) simulator in Section III. First, the properties of single monopoles and single PIFAs with different locations on the chassis are examined. The results indicate that, for a given location on the chassis, different types of antennas localize the chassis excitation currents to different extents. This insight can be used to improve the isolation between multiple antenna elements. Second, multiple antenna cases are studied to investigate the effects of chassis current localization on isolation for different antenna combinations. In Section IV, performance tradeoff analyses of different antenna locations on the mobile chassis is presented with respect to bandwidth, efficiency, correlation, effective diversity gain and capacity. Based on the analysis, three dual-antenna prototypes were fabricated, and their experimental results are presented in Section V. Finally, some conclusions are given in Section VI.

II. CHARACTERISTIC MODE ANALYSIS

The mode of an oscillating structure is a pattern of motion in which the entire structure oscillates sinusoidally with the same frequency. The frequencies of the modes are known as their natural frequencies or resonant frequencies. A physical object has a set of modes that depend on its structure, materials and boundary conditions.

The characteristic mode analysis is a method used in electromagnetics, which gives insight into the potential resonant characteristics of a structure by finding and examining the inherent modes of the structure. The existence of the modes is independent of the excitation. However, different kinds of excitations or excitations at different locations/frequencies are expected to excite different modes, to satisfy different requirements. From this perspective, the characteristic mode analysis can provide physical insight into the fundamental electromagnetic properties of scattering objects and valuable information on antenna design.

The theory of characteristic mode was first introduced by Robert Garbacz in [24] and later refined by Roger Harrington in [19] and [25].

Considering a conducting body with surface *S*, an external electric field (or voltage) $\vec{E}^{ex}$ can induce a surface current J_s on it. This surface current will further generate a scattered field $\vec{E}^{s}$. According to the boundary condition, the tangential component on the surface of the conducting body satisfies

$$(\vec{E}^{ex} + \vec{E}^{s})_{\tan} = 0 \ . \qquad (1)$$

Equation (1) can be rewritten with an operator $L(\bullet)$

$$[L(J_s)]_{\tan} - \vec{E}^{ex}_{\tan} = 0, \tag{2}$$

where the term $-L(J_s)$ can be considered as the electric field intensity on the surface due to the surface current J_s. The operator $L(\bullet)$ has the dimension of impedance, and the following notations are hence introduced

$$Z(J_s) = [L(J_s)]_{\tan}, \tag{3}$$

$$Z(J_s) = R(J_s) + j\,X(J_s). \tag{4}$$

Following the approach in [19], characteristic mode is defined by the eigenvalue equation expressed as

$$X(J_{s,n}) = \lambda_n R(J_{s,n}). \tag{5}$$

In our work, this linear equation is transformed to matrix equation using the method of moments (MOM) [26]. The MOM relies on Rao-Wilton-Glisson (RWG) edge elements. The surface of the metal antenna is divided into separate triangles (see Fig. 1(d)). Each pair of triangles, having a common edge, constitutes the corresponding RWG edge element. These RWG edge elements correspond to the division of the antenna into small elementary electric dipoles. In this sense, the impedance matrix **Z** describes the interaction between different elementary dipoles. If the edge elements m and n are treated as small electric dipoles, the element $\mathbf{Z}_{mn}$ describes the contribution of dipole n to the electric current of dipole m, and vice versa. This contribution is calculated through electric field integral equation (EFIE). The size of impedance matrix is equal to the number of the edge elements. With the matrix equation, the characteristic eigenvalues (λ_n), eigenvectors ($J_{s,n}$) and characteristic electric fields of the chassis are calculated with Matlab.

The chassis, with the dimensions of a typical candybar-type mobile phone (100 mm × 40 mm), is modeled by a perfectly conducting board. Its eigenvalues over a frequency range from 0.5 GHz to 1.5 GHz are calculated in Matlab, and shown in Fig. 1(a). A scattered plot is employed to generate the figure and the chassis is meshed with 736 edge elements. As known from [19], the smaller the magnitude of λ_n, the more important the mode is for radiation and scattering problems, and $\lambda_n = 0$ corresponds to a resonant mode. As observed from Fig. 1(a), the lowest resonant frequency of our chassis is 1.35 GHz. The mode in our work is numbered according to the order of occurrence of its resonant frequency. The lower the resonant frequency, the smaller is the mode number. The mode number of zero (or λ_0) denotes a non-resonant mode.

To highlight the respective roles of characteristic modes and external excitation in chassis radiation, the total current on the surface of a conducting body can be expressed by the eigenvectors as

$$J_s = \sum_n \frac{V_n^{ex} J_{s,n}}{1 + j\lambda_n}. \tag{6}$$

There are two factors determining the contribution of a certain (or nth) mode to the total current distribution [23], i.e., the modal-excitation coefficient

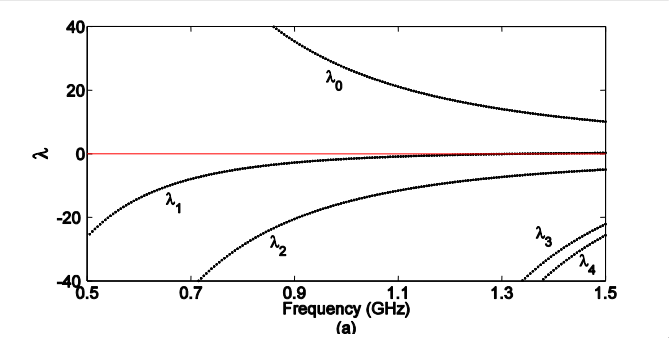

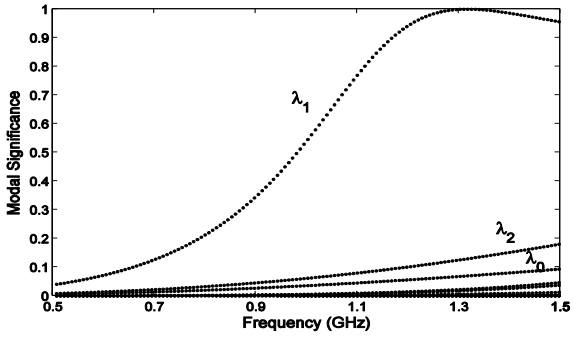

(b)

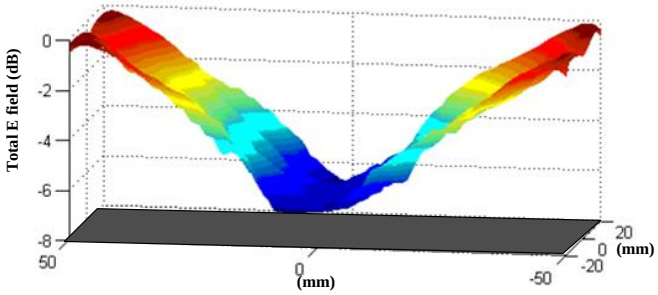

(c)

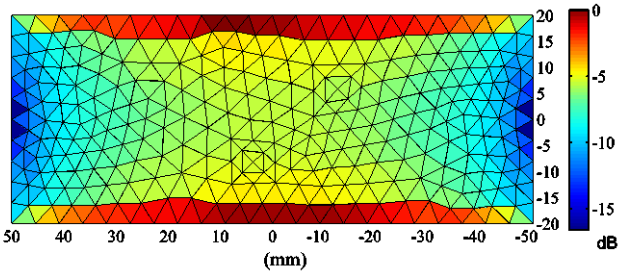

(d)

Fig. 1. (a) The eigenvalues against frequency for the mobile chassis; (b) The modal significance (MS) against frequency for the mobile chassis; (c) The normalized magnitude of the total electric field of the first characteristic mode of the chassis at 1.35 GHz; (d) The normalized eigenvector of the first characteristic mode of the chassis at 1.35 GHz.

$$V_n^{ex} = \left\langle J_{s,n}, E^{ex} \right\rangle = \oint_n J_{s,n} \bullet E^{ex} ds. \tag{7}$$

and the modal significance (MS)

$$\mathrm{MS} = \left| \frac{1}{1 + j\lambda_n} \right|. \tag{8}$$

Whereas V_n^{ex} accounts for the external excitation, including the influence of its position, magnitude and phase, MS represents the inherent normalized amplitude of the characteristic modes. External excitation (e.g., port excitation) will not change the characteristic modes of the conducting body; however, its location on the structure is very important for the excitation of certain characteristic mode(s).

The MS of each mode of the chassis is presented in Fig. 1(b). It can be observed that the first mode (λ_1) is dominant at 1.35 GHz, while the other modes only contribute slightly to the current distribution (with MS < 0.2). Thus, at the frequency band around 1 GHz, we focus mainly on the first mode of the chassis and its interaction with the antenna on the chassis.

The characteristic total electric field of the first mode on a plane 5 mm above the chassis is evaluated at 1.35 GHz, and shown in Fig. 1(c). The field is normalized to the maximum value and presented in dB scale. The field corresponds to that of a flat half-wavelength dipole [21]. It can be observed that the electric field is stronger at the edges, especially at the corners, whereas it becomes very weak at the center of the chassis. For the single antenna case, this insight reveals that the characteristic mode can be most efficiently excited when a voltage (a port excitation) is applied at the edge or at the corner. However, if multiple antennas at the same or closely similar frequencies are integrated on the same chassis, the locations of the antennas should be carefully considered. Concerning the mutual coupling, if the antenna (e.g., a dipole) is responsive to electric field, the place where the electric field is strong is not a good location for more than one such antenna. On the other hand, if the antenna (e.g., a small loop) responds mainly to magnetic field, the place with strong magnetic field is likewise not a good location for more than one such antenna. Since most types of mobile terminal antennas base their mechanisms on electric field, we focus on electric field in this paper.

The normalized eigenvector (i.e., characteristic current) of the first characteristic mode of the chassis is presented in Fig. 1(d). A sinusoidal current distribution along the length of the chassis is observed, which shows that the length of the chassis is approximately one half of a wavelength at the first resonant frequency. This current distribution is similar to that calculated in the EM simulator for an excited monopole on the chassis (see Fig. 7(a) and Fig. 8(c)).

Once antennas are implemented on the chassis, the electrical length of the chassis is correspondingly increased, and its resonant frequency will be further reduced, making it closer to 900 MHz. To verify this hypothesis, the eigenvalues of the 100 mm × 40 mm chassis with a planar slot monopole [27] etched in it are calculated in Matlab and shown in Fig. 2(a). The dimensions of the slot monopole are presented later in the paper (see Fig. 8(b)). The lowest resonant frequency of 1.06 GHz is observed in the figure. Moreover, when the antenna is excited with a feed, its resonant frequency can be slightly changed. Another observation from Fig. 1(a) and Fig. 2(a) is that the first resonance of the chassis, with and without the slot monopole element, is relatively wideband, which appears to substantiate the findings of [17] that the chassis size is often less important than the locations of the antenna element and its feed in determining single antenna performance.

The characteristic total electric field of the first mode of the slot monopole is evaluated at 1.06 GHz and presented in Fig. 2 (b). As expected, the trend of the electric field is similar to that of the chassis-only case in Fig. 1(c). Due to the resonance of the slot monopole at 1.06 GHz, the positions of maximum and minimum electric fields are slightly changed. The maximum electric field occurs at the edge with the slot monopole, and the minimum value shifts slightly from the center towards the monopole side. From the perspective of isolation, the best location for another antenna should be in the region of the minimum electric field so that the characteristic mode will not be shared simultaneously by two antenna elements. This principle will be further analyzed and verified by the antenna simulations in the following section.

The chassis with slot monopole is also simulated in the frequency domain solver of CST Microwave Studio, with the monopole excited by a lumped port. The total electric field is similar to the characteristic electric field in Fig. 2(b), and is thus not included here.

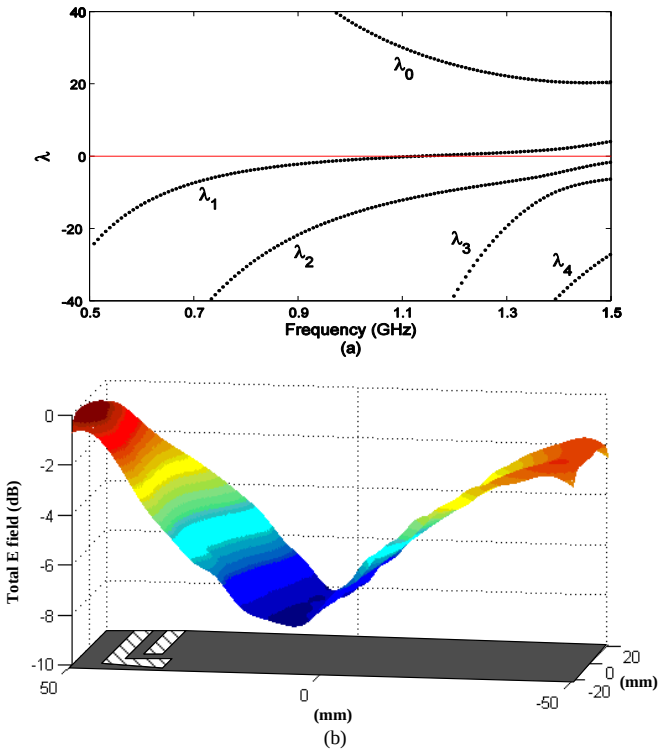

Fig. 2. (a) The eigenvalues against frequency for the mobile chassis with a slot monopole; (b) The normalized magnitude of the total electric field of the first characteristic mode of the slot monopole at 1.06 GHz.

III. Antenna Simulation

In this section, according to the results of the characteristic mode analysis, the excitation ports are applied to different locations of the chassis. Full-wave antenna simulations are carried out in the frequency domain using the CST Microwave Studio software. Single monopole antenna and single PIFA cases are studied first, to identify the degree to which the

radiation properties are influenced by different antenna types and locations. Our choice is based on the fact that PIFAs and low profile variants of monopole antennas are the most commonly used antenna types in today's mobile terminals. Based on these results, multiple antenna cases are then analyzed. The size of the mobile chassis is 100 mm × 40 mm, which is identical to that in the previous section. The chassis consists of a 0.1 mm top copper layer and a 1.55 mm bottom FR4 layer with a permittivity of 4.7 and a loss tangent of 0.015. All antennas, except the top-loaded monopoles, are designed for dual-band (900/1900 MHz) operation. However, the focus of the study in this and the following sections are on the 900 MHz band. Note that even though the dimensions of the monopoles and PIFAs used in the paper are provided, they are specific to a given antenna location and are slightly tuned to ensure good impedance matching (i.e., reflection coefficient S_{11} < –12 dB) for other locations.

A. Single Antenna Cases

In this sub-section, four single antenna cases are studied: quarter-wavelength top-loaded monopole at the center (MC) or edge (ME) of the chassis, and PIFA at the center (PC) or edge (PE) of the chassis. The geometry of the monopole and its location on the mobile chassis are shown in Fig. 3. Perfect electric conductor (PEC) is assumed as the antenna material. The top load (i.e., a circular plate with thickness of 0.1 mm) is used to help match the monopole and slightly reduce its height, without changing the radiation characteristics. The monopole is first put at the edge of the chassis, and then moved to the center with its dimension unchanged. The same monopole antenna on an infinite ground plane (MIG) is also presented for comparison. All the antennas are well matched at 0.92 GHz.

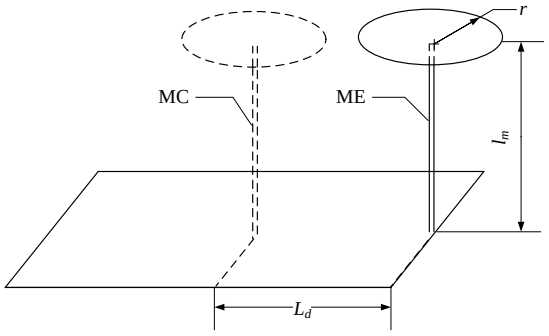

Fig. 3. Geometry of quarter-wavelength top-loaded monopole and its locations on the chassis in the single antenna case. The dimensions are: l_m = 36 mm, r = 11 mm, L_d = 50 mm. Diameter of the wire is 1 mm.

Real and imaginary parts of the simulated input impedance and the magnitude of the reflection coefficients are shown in Figs. 4(a) and 4(b), respectively. As can be seen in Fig. 4(a), the input impedances of MC and MIG share a similar trend, whereas that of ME is quite different. As explained in the previous section, the characteristic mode for the eigenvalue λ_1 is easily excited when the antenna is located at the edge of the chassis [13], since the resonance of chassis is close to 0.92 GHz. The high radiation resistance in the ME case is mainly due to the excitation of the characteristic mode, which increases the bandwidth dramatically (see Fig. 4(b)).

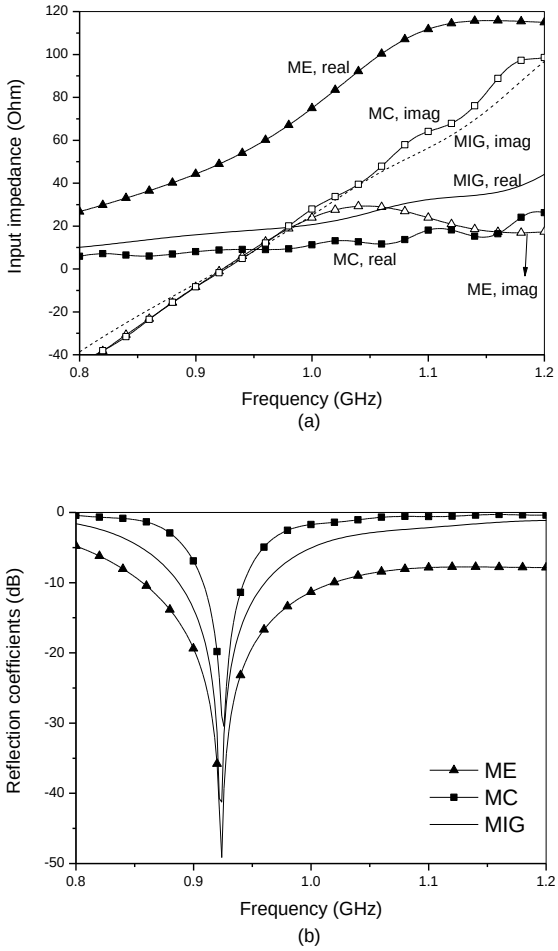

Fig. 4. (a) Input impedances and (b) reflection coefficients of the simulated top-loaded monopole at different locations with finite/infinite ground plane.

The PIFA cases are studied in a similar way. The geometry and different locations of the single PIFA are shown in Fig. 5. The PIFA is integrated onto a hollow carrier (i.e., the shaded regions), which is commonly used in mobile phones. The simulated carrier has a thickness of 1 mm, a permittivity of 2.7 and a loss tangent of 0.007. To further separate the effect of the edge from that of the characteristic mode, one more case is included, i.e., the PIFA in the center rotated by 90° and moved to the longer edge of the chassis (RPC), as illustrated in Fig. 5(b). A PIFA on an infinite ground plane (PIG) is used for comparison. From Fig. 6(a), it can be observed that the input impedance of PE is notably different from all other cases. With the help of the chassis, both the input resistance and reactance become larger in amplitude and flatter over frequency. As a result, the bandwidth is significantly improved (see Fig. 6(b)).

To confirm that the larger bandwidth of PE is primarily the result of characteristic mode excitation, rather than due to the PIFA being at the chassis edge, the effect of the edge can be examined by comparing the bandwidths of RPC and PC. Since the difference in bandwidth between the two cases is negligible, it can be concluded that the edge effect is unlikely to have contributed to the wideband behavior in the PE case.

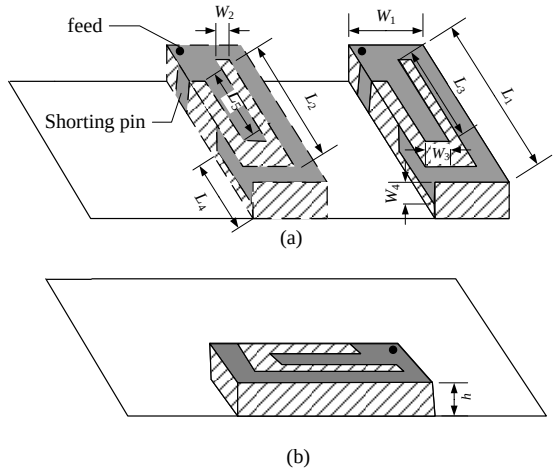

Fig. 5. Geometries of the PIFA and its locations on the chassis in the single antenna case. The dimensions are: L_1 = 40 mm, L_2 = 30.2 mm, L_3 = 26.2 mm, L_4 = 11 mm, L_5 = 22.8 mm, W_1 = 17 mm, W_2 = 4 mm, W_3 = 5 mm, W_4 = 4 mm, h = 6 mm.

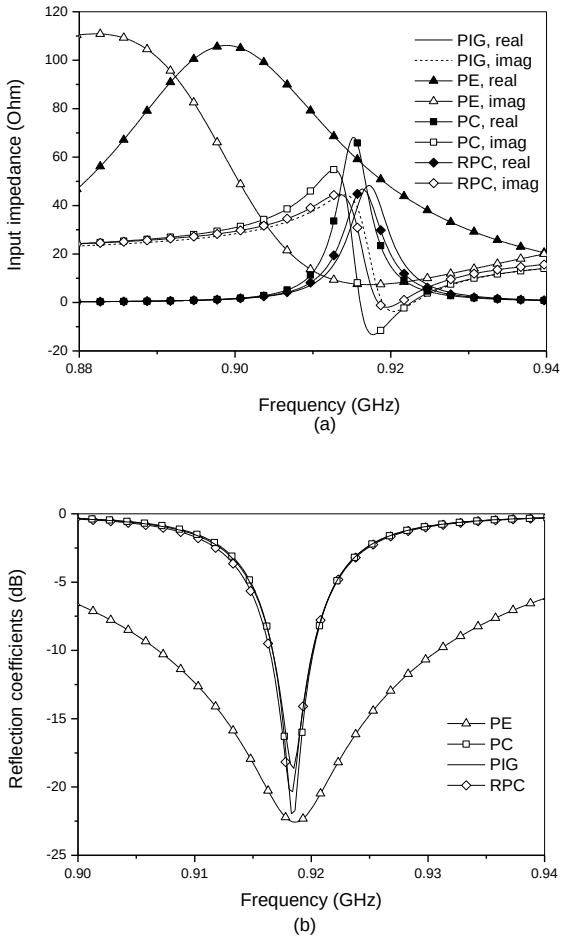

Fig. 6. (a) Input impedances and (b) reflection coefficients of the simulated PIFA at different locations with finite/infinite ground plane.

In order to gain further insights into the influence of chassis on the characteristics of monopole and PIFA at different locations, normalized current distributions are given for four distinct cases in Fig. 7. The normalization is performed against the peak current in each case. Two conclusions can be drawn from the current distributions. First, when the antenna is at the short edge, regardless of its type, the characteristic mode of the chassis is excited (see Figs. 7(a) and 7(c)), and the current is distributed over the whole chassis. This current distribution is similar as the eigenvector of the first characteristic mode (see Fig. 1(d)), especially for the ME case. This further verifies the strong excitation of the first characteristic mode. When the antenna is at the center, the current is more confined to the immediate vicinity of the antenna. By comparing ME and MC in Fig. 4(b) and PE and PC in Fig. 6(b), the characteristic mode excitation is observed to offer significantly larger bandwidths for the ME and PE cases than for the MC and PC cases, respectively. Second, the current of PIFA is more localized than that of monopole at either the center or the short edge. In other words, its radiation depends less on the chassis than that of the monopole. Therefore, in addition to the concept of characteristic mode, localization of chassis current is also important in determining the isolation between antenna elements: The more localized the induced current on the chassis, the less is the current that couples from one antenna port into other antenna port(s). Nonetheless, it should be noted that an antenna with more localized current is an indication of a smaller effective radiator, which inevitably leads to a reduction of bandwidth. This aspect can be seen in the narrower bandwidths of the PC and PE cases, relative to the MC and ME cases, respectively. Further analysis of the localized current phenomenon is provided in Section IV.

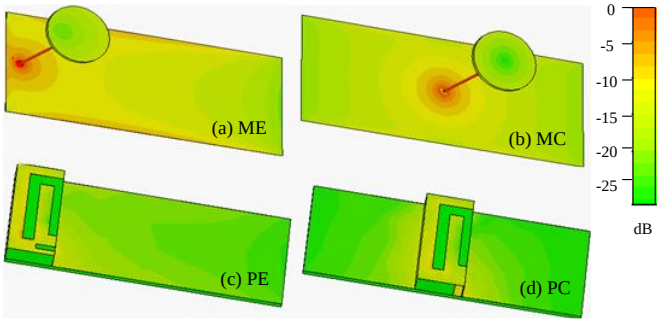

Fig. 7. Normalized magnitude of current distributions for: (a) monopole at the edge, (b) monopole at the center, (c) PIFA at the edge, (d) PIFA at the center.

B. Dual-Antenna Cases

In this subsection, different combinations of antenna types, including monopole-monopole (MM), PIFA-PIFA (PP) and monopole-PIFA (MP), and antenna locations (at the edge(s) and at the center) are studied to shed light on the effect of characteristic mode and current localization on the isolation level between two antenna elements on the chassis.

In all the simulations, two antennas (of monopole(s) and/or PIFA(s)) are integrated onto the same chassis of dimensions 100 mm × 40 mm. One antenna is fixed at one short edge, and the other antenna is placed either at the opposite short edge or at the center. A planar slot monopole [27] rather than the top-loaded monopole is used as the fixed monopole at the edge, considering antenna dimensions and matching problem. The schematic drawing of the antenna setup and the geometry of the

slot monopole are shown in Fig. 8. The slot monopole is etched into the ground plane on a substrate of FR4. It is fed by a microstrip line (i.e., the dashed line in Fig. 8(b)) on the other side of the substrate. The width of both of the slots is W_S = 5 mm. Good antenna matching is achieved by optimizing the value of D_f. The radiation pattern and polarization of the slot monopole are only slightly different from those of the top-loaded monopole when they are implemented on the mobile chassis, since they both strongly excite the chassis, which acts as a radiator. The normalized current distribution when the slot monopole is excited is shown in Fig. 8(c). It is observed that the degree of chassis excitation is similar as that when the top-loaded monopole is used (Fig. 7 (a)).

The simulation results are shown in Fig. 9. It is interesting to note that, in all dual-antenna cases, the isolation improves when one antenna is moved to the center (i.e., the two antennas become closer). This phenomenon contradicts with intuition and the common knowledge on the relationship between antenna separation distance and port isolation. However, this situation can be explained by the characteristic mode analysis in Section II and the single antenna simulations above. When the antenna elements are at the two edges, they excite the chassis simultaneously. Since the chassis not only functions as a ground plane, but also as the main radiator for both antenna elements, the port isolation must be low. The mutual coupling, in this case, not only comes from the field in free space and the conventional ground plane current, but also from the radiation of the shared chassis. Thus, it is difficult to achieve angle and polarization diversity for the antenna elements in this setup. When one antenna is moved to the center, the chassis is not efficiently excited, and hence the current is more localized. The chassis is only utilized as the main radiator by the antenna (either the monopole or the PIFA) at the chassis edge. Consequently, angle and polarization diversity can be more easily achieved for the edge-and-center placement, which enhances the isolation.

It is also observed that different dual-antenna combinations offer different degrees of improvement in isolation, when considering different placement options of a given combination. The most dramatic improvement is achieved in the M-P combination, in which the monopole is the fixed antenna and the PIFA is either at the edge or the center of the ground plane. This improvement is mainly due to the localized current achieved by the PIFA when it is at the center. Another reason is that employing antennas of different types can reduce mutual coupling to some extent by taking advantage of angle diversity in their radiation patterns. The improvement in the isolation of the P-P combination is better than that of the M-M combination, and this is attributed to the localized current behavior of the PIFAs, as shown in Figs. 7(c) and 7(d) for the single antenna cases.

By taking into consideration both characteristic mode and current localization, isolation of over 10 dB is achieved in the M-P combination, which can be considered low enough for terminal applications involving frequencies lower than 1 GHz. In addition, the antennas are easy to design and tune, since no additional matching or decoupling structures are needed.

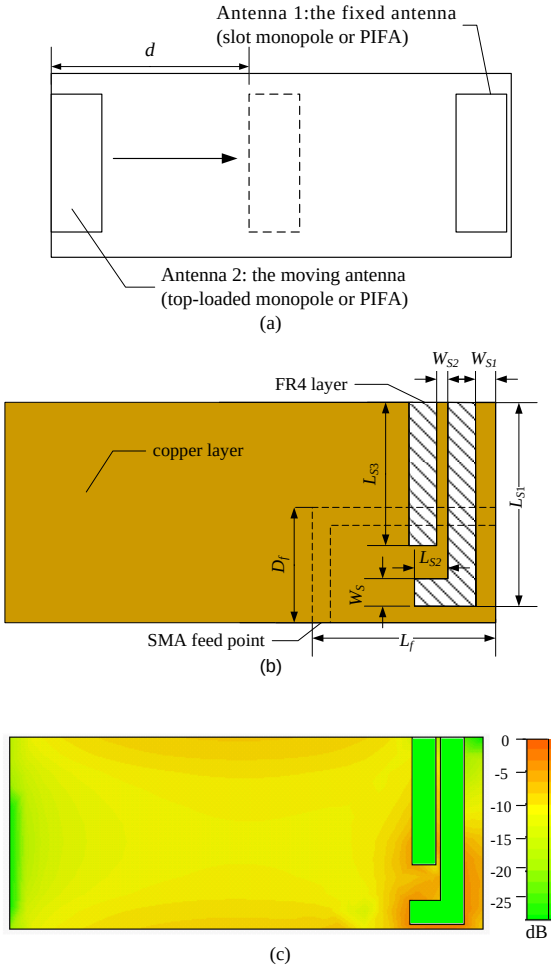

Fig. 8. (a) The schematic drawing of the locations of antennas in the dual-antenna case. (b) The geometry of the slot monopole. The dimensions are: L_{S1} = 39 mm, L_{S2} = 6 mm, L_{S3} = 24 mm, W_S = 5 mm, D_f = 18 mm, L_f = 30 mm, W_f = 2.8 mm, W_{S1} = 4 mm, W_{S2} = 1 mm. (c) The normalized current distribution of the slot monopole on the chassis.

From the perspective of bandwidth, the monopole antenna performs well, whereas the bandwidth of the PIFA is narrow, especially when it is placed at the center of the chassis. Thus, the P-P combination is impractical, even though the isolation is improved for the center-and-edge placement, in comparison to the edge-and-edge placement. The M-M combination is likewise impractical, due to the difficulties in implementing a low profile monopole at the center: Its dimensions tend to be large and it is difficult to achieve good matching. In addition, the isolation between the monopoles is only 7 dB at the center frequency. Consequently, the M-P combination is more attractive for mobile terminal applications. As has been suggested in [12], the monopole can be used as the main antenna to cover both downlink and uplink frequencies, whereas the narrowband PIFA can be used as a diversity antenna for only the downlink frequencies.

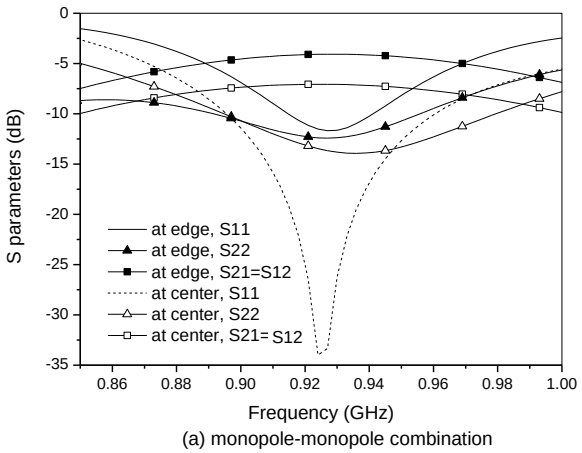

(a) monopole-monopole combination

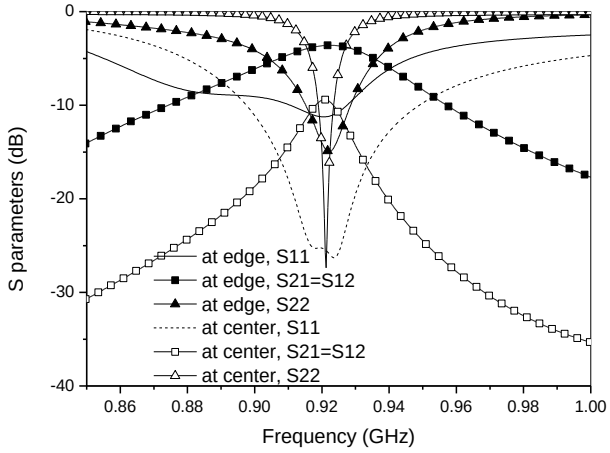

(b) monopole-PIFA combination with PIFA at the edge or the center of the ground plane

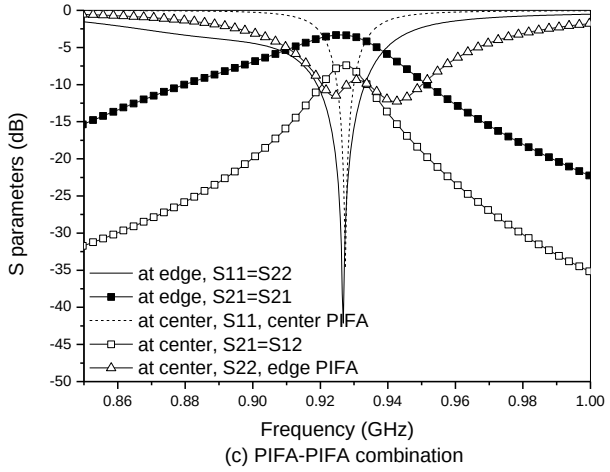

(c) PIFA-PIFA combination

Fig. 9. The simulated scattering parameters of dual-antenna terminals with different locations and combinations of antenna elements: (a) M-M combination, (b) M-P combination, with PIFA at the edge or the center of the ground plane, and (c) P-P combination.

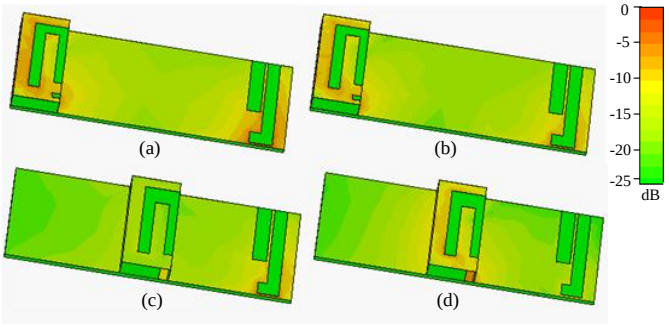

Fig. 10. Normalized magnitude of current distributions for the M-P case: (a) PIFA at the edge, monopole excited, (b) PIFA at the edge, PIFA excited, (c) PIFA at the center, monopole excited, (d) PIFA at the center, PIFA excited.

C. Discussions

For the M-P combination, normalized current distributions are shown in Fig. 10. In Figs. 10(a) and 10(b), when the two antennas are at the edges, the characteristic mode is easily excited, resulting in strong electric fields at the two edges. Therefore, if one antenna is excited, the other antenna is also strongly excited, which leads to poor isolation. In Fig. 10(c), the PIFA is influenced to some extent, since the characteristic mode is efficiently excited by the monopole; whereas in Fig. 10(d), when the PIFA is excited, due to its localized current, the chassis acts primarily as a common ground rather than a radiator. Thus, good isolation is achieved.

Rather than only the slot monopole, different monopole types, including the most frequently used folded monopole (such as the monopole in [12]), have also been simulated. The trend of isolation enhancement is the same when the PIFA moves away from the edge to the center location. The slot monopole is used in our work due to the convenience of fabrication and matching. Concerning the bandwidth of PIFA, we note that the PIFA can be made tunable to cover different bands according to different requirements.

IV. Tradeoff Analysis Of Dual-Antenna Terminals

In this section, the performance tradeoffs of dual-antenna terminals are investigated with respect to different locations of the PIFA on the chassis for the M-P combination in Section III-B. The different PIFA locations are meant to induce different levels of characteristic mode excitation. The PIFA is moved gradually from the edge to the center, in steps of 5 mm. d is the distance between the PIFA location and the edge (see Fig. 8(a)). When the PIFA is at the edge, d = 0 mm.

The relative bandwidth of the two antennas is shown in Fig. 11(a). Here, the relative bandwidth is defined as the ratio of the 6 dB impedance bandwidth to the center frequency. It is obvious that the bandwidth of the monopole is much wider than that of the PIFA, and it is almost constant regardless of the PIFA's location. That is one reason that the monopole is used as the main radiator in the M-P combination. The relative bandwidth of the PIFA falls quickly when it is moved away from the edge, since the chassis no longer contributes significantly to the PIFA's radiation. Indeed, it is observed that the bandwidth is almost unchanged when the PIFA is moved around the center location.

The efficiencies of both antennas, including the radiation efficiency at the center frequency and the average total efficiency over a given bandwidth, are presented in Fig. 11(b). Overall, the efficiencies of both antennas increase when the PIFA is moved from the edge to the center. The radiation efficiency η_{rad} is analyzed first. The highest radiation efficiency of the PIFA appears at the edge and decreases by 15% when it is moved to the center. This is because the chassis excitation helps to increase the radiation resistance of the PIFA at the edge (see Fig. 6(a)).

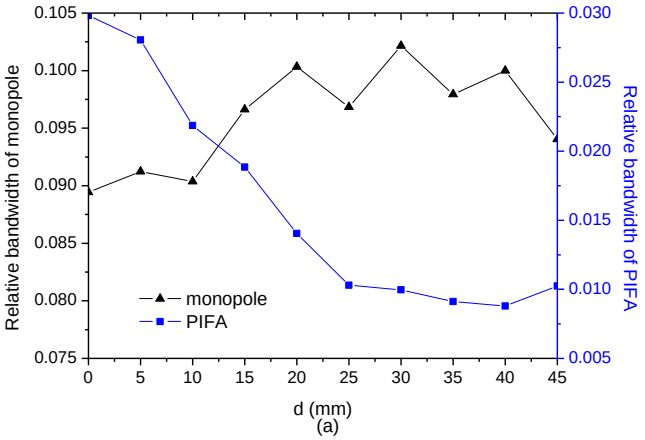

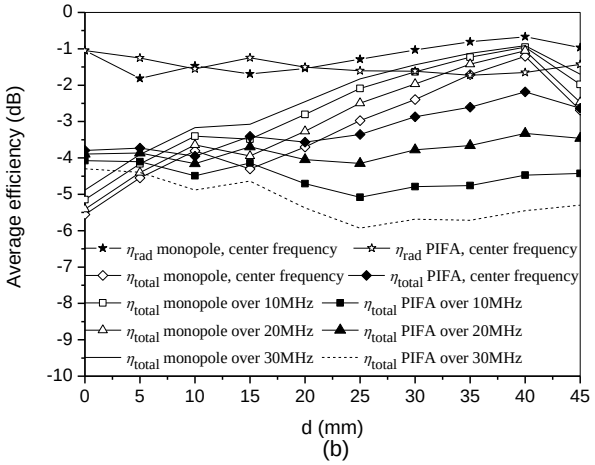

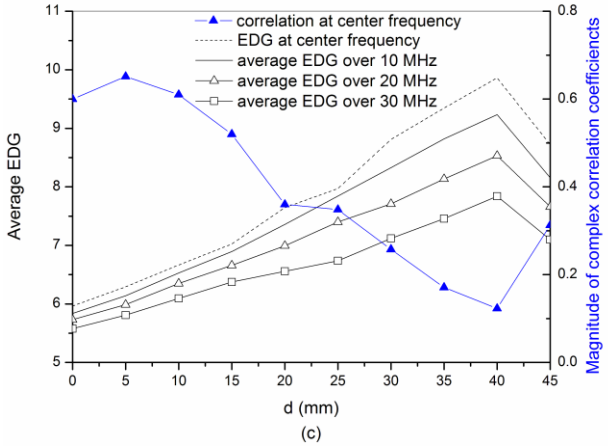

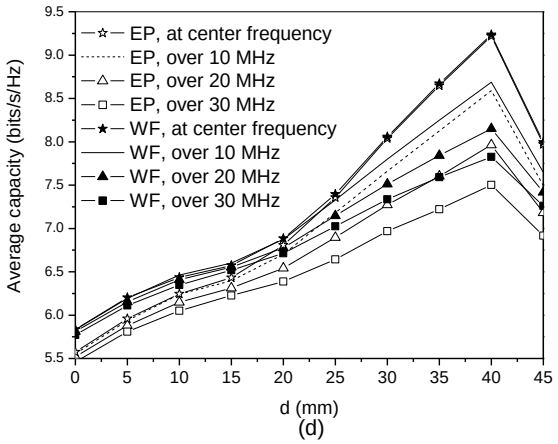

Fig. 11. Performance tradeoffs of the dual-antenna terminal with respect to the PIFA location in terms of the (a) relative bandwidth, (b) average efficiency, (c) magnitude of complex correlation coefficient and average EDG, and (d) average channel capacity.

According to expression

$$\eta_{\text{rad}} = \frac{R_{\text{r}}}{R_{\text{r}} + R_{\text{L}}}\ , \tag{9}$$

where R_{r} is the radiation resistance and R_{L} represents the conduction-dielectric losses (which is almost constant over the given range of frequency), efficiency can be high if the radiation resistance is large. For the monopole, the radiation efficiency does not change appreciably, since it always takes advantage of the chassis to radiate efficiently.

The total efficiency is given by

$$\eta_{\text{total}} = \eta_{\text{rad}}\left(1-\left|S_{11}\right|^2-\left|S_{21}\right|^2\right). \tag{10}$$

When the PIFA is at the edge, the total efficiencies are relatively low for both antennas, due to strong mutual coupling (i.e., large S_{21}). As the PIFA moves away from the edge, the total efficiency of the monopole increases greatly, regardless of the bandwidth within which it is calculated. The total efficiency of the PIFA increases as it is moved towards the center of the chassis, if it is only measured at the center frequency. However, the trend changes when it is measured within a 30 MHz bandwidth, because of its narrowing impedance bandwidth with d (see Fig. 11(a)). Therefore, the optimal position of the PIFA can be different, depending on the efficiency bandwidth requirement.

Correlation coefficient and diversity gain are important metrics for evaluating the performance of multiple antenna systems. Fig. 11(c) presents the magnitude of complex correlation coefficients at the center frequency, together with the average effective diversity gain (EDG) over the given bandwidths. EDG [12] is defined by

$$\text{EDG} = \text{DG} \times \eta_{\text{best branch}}\ , \tag{11}$$

where $\eta_{\text{best branch}}$ is the total efficiency of the antenna with the highest efficiency and DG is the (apparent) diversity gain. In this paper, DG is calculated with the maximum ratio combining (MRC) method and taken at 1% probability. All the EDGs (over different bandwidths) improve as the PIFA is moved

towards the center. Though the improvement becomes less obvious when calculated over a larger bandwidth, a minimum enhancement of 2.3 dB can be observed within a bandwidth of 30 MHz. The smallest correlation coefficient of 0.11 is achieved when d = 40 mm, which corresponds to the PIFA structure at nearly the center location of the chassis.

The average channel capacity calculated under the equal power (EP) and water-filling (WF) conditions for SNR = 20 dB is presented in Fig. 11(d). The WF procedure is performed over the antenna elements. The Kronecker model and uniform 3D angular power spectrum (APS) is assumed. There is no correlation between the (base station) transmit antennas, whereas the (mobile terminal) receive antennas are correlated according to their radiation patterns and the 3D APS. The capacity is averaged over 10,000 i.i.d. Rayleigh realizations at each frequency. The channels are normalized with respect to the i.i.d. Rayleigh case, which means that the correlation, total efficiency and power imbalance (efficiency imbalance) are taken into account in the capacity evaluation. As reference cases, the average capacities for the 2 × 2 i.i.d. Rayleigh channel with the EP and WF schemes are 11.29 bits/s/Hz and 11.32 bits/s/Hz, respectively.

Similar to the figure of EDG, the largest capacity is achieved when d = 40 mm, due to the low correlation and high efficiency of the monopole when the PIFA is at the center. Because of the PIFA's narrow bandwidth, the power imbalance becomes serious at frequencies away from the center frequency. This means that one antenna (or spatial channel) is not efficiently used, and thus the average channel capacity decreases. In general, the average capacity increases when the PIFA is moved to the center, and the improvement is less obvious with an increase in bandwidth. For the WF case, the power imbalance is accounted for in the transmit power allocation, so the channel is more efficiently used than in the EP case. Thus, the capacity improvement of WF over EP increases with power imbalance, which increases with bandwidth.

V. Experiments and Discussions

The PIFAs and monopoles used by the dual-antenna prototypes in Section IV are dual-band antennas and they cover both 880 MHz – 960 MHz and 1880 MHz – 1990 MHz frequency bands. Three prototypes are fabricated for the slot monopole at one edge and (i) the PIFA at the opposite edge, (ii) the PIFA at the center, and (iii) the rotated PIFA at the center (see Fig. 12). The scattering (or S) parameters are measured with a vector network analyzer and shown in Fig. 13. The isolation is improved from 5 dB to 13 dB when the PIFA is moved to the center. As a tradeoff, the bandwidth of the PIFA is reduced from 30 MHz to 12 MHz. In practice, PIFA can be made tunable to cover different bands according to the given requirement. The scattering parameters are almost unchanged when the PIFA is rotated by 90 degrees.

The far field electric field patterns are measured in a Satimo Stargate-64 antenna measurement facility. For cases (i) and (ii), the patterns at the center frequency of the low band are shown in Figs. 14 and 15, respectively. The patterns of the case (iii) (as illustrated in Fig. 12(c)) are not included here, because the pattern of the monopole is similar to that of the monopole in Fig. 12(b), and the pattern of PIFA is similar to that of the PIFA in Fig. 12(b) after a 90° rotation. The measured patterns agree well with the simulated ones. The slight differences are caused by influences of the feeding cables. The correlations calculated from the measured patterns are 0.5, 0.18, and 0.19, respectively, for the three prototypes in Fig. 12. Due to some cable influence [12] and practical difficulties in measuring antennas with very high correlation, the measured correlation for the case with the antennas at the edges (i.e., Fig. 12(a)) is slightly lower than the simulated one.

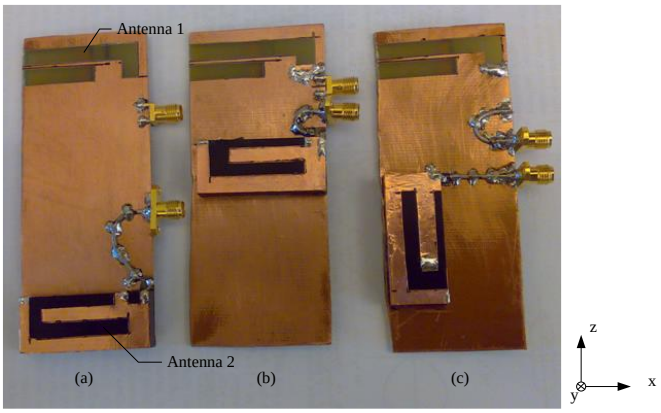

Fig. 12. Prototypes with the slot antenna at one edge and (a) the PIFA at the opposite edge, (b) the PIFA at the center, (c) the rotated PIFA at the center.

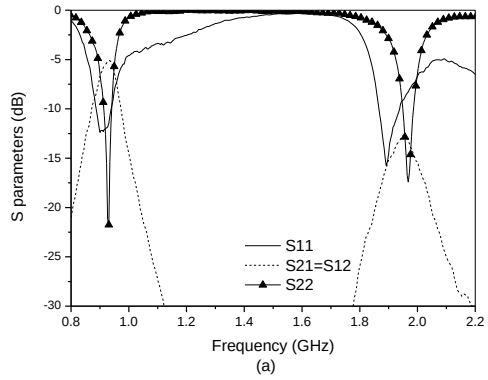

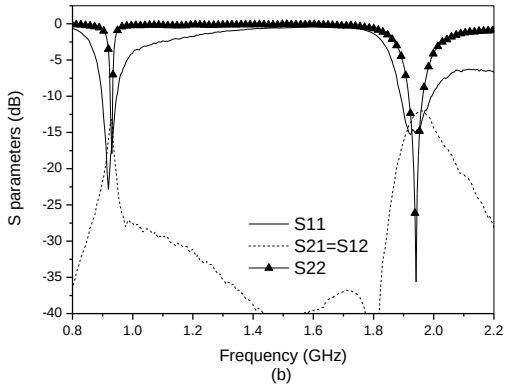

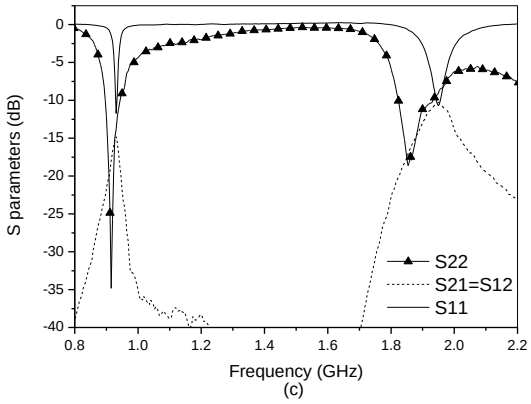

Fig. 13. Measured scattering parameters for the slot antenna at one edge and (a) the PIFA at the opposite edge (b) the PIFA at the center and (c) the rotated PIFA at the center.

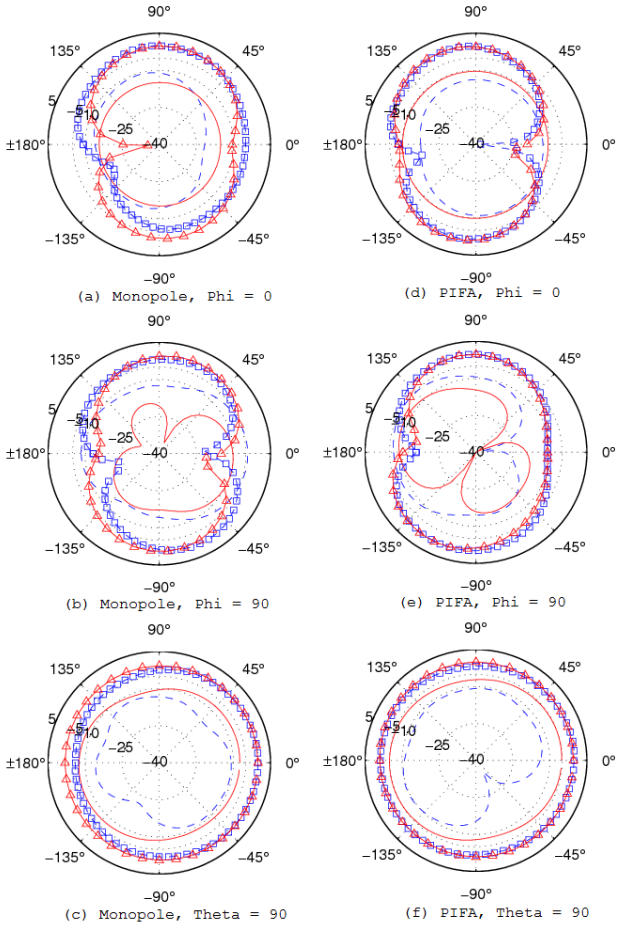

Fig. 14. Simulated and measured antenna patterns for the antenna system in Fig. 12(a): (—) simulated *E*(Phi), (– –) measured *E*(Phi), (-▲-) simulated *E*(Theta), (-□-) measured *E*(Theta).

The measured efficiencies over two operating bands are shown in Fig. 16. In general, the measured efficiencies are slightly lower than the simulated ones due to fabrication and experimental tolerances. At the low frequency band, when the PIFA is at the edge, the efficiencies of the monopole are relatively low around the center frequency due to high mutual coupling. When the PIFA is at the center, the efficiencies of monopole approach that of a single monopole on mobile chassis, whereas the PIFA efficiency becomes more narrowband. At the high frequency band, the efficiencies of the monopole are around 70%, since the coupling is not significant. The highest efficiency of the PIFA is 75%, and good efficiency is kept in downlink band. All these results agree well with simulations.

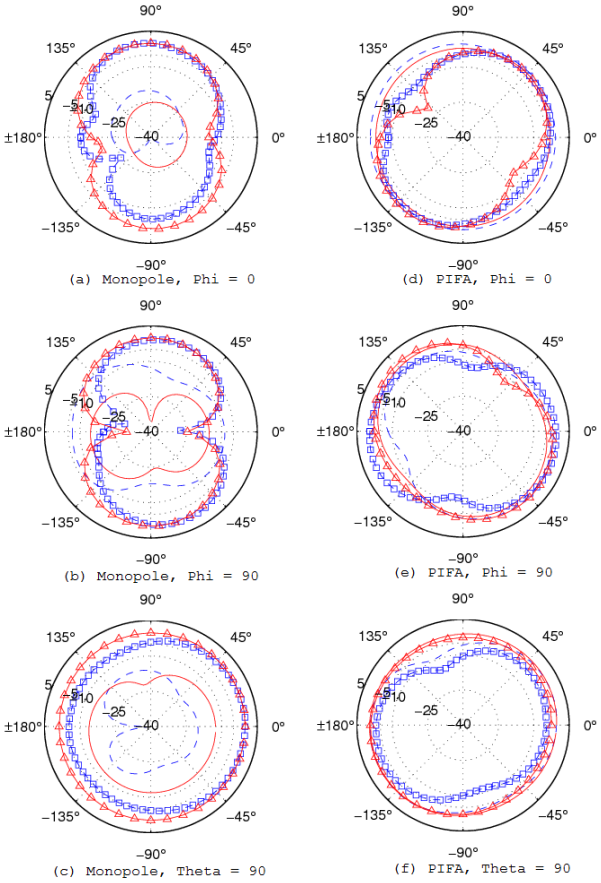

Fig. 15. Simulated and measured antenna patterns for the antenna system in Fig. 12(b): (—) simulated *E*(Phi), (– –) measured *E*(Phi), (-▲-) simulated *E*(Theta), (-□-) measured *E*(Theta).

VI. Conclusions

In this work, fundamental design tradeoffs of multiple antennas on a mobile chassis are studied in the context of characteristic mode excitation and the ability of antennas to localize chassis currents. The goal is to provide useful information and a design framework for optimal implementations of multiple antennas on a mobile chassis according to different requirements.

The results for the 900 MHz band show that whereas the PIFA has more localized currents than the monopole, especially when it is at the center of the chassis, it is the monopole-PIFA combination that achieves the best isolation of over 10 dB (13 dB for the measured case). Utilizing characteristic mode and chassis current localization in the design of multiple antennas has the advantage of not requiring any additional matching or decoupling structures. Three prototypes are fabricated and measured to test three selected cases, and the results are found to be in good agreement with those from simulations.

Since a mobile terminal user can significantly influence the results obtained in this study, the effects of user on antenna-chassis interaction is an interesting topic for future work.

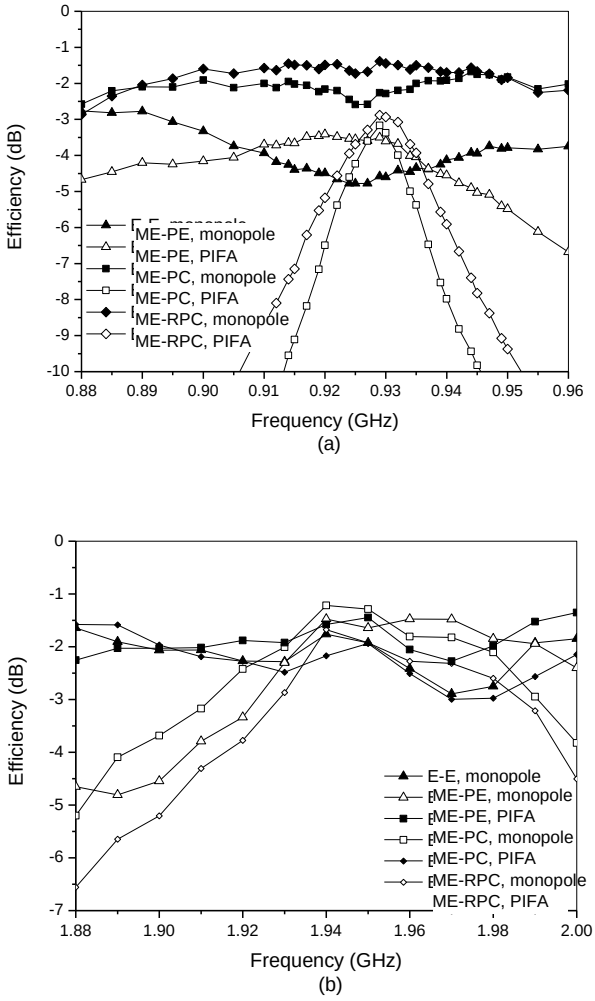

Fig. 16. Measured efficiencies (a) low frequency band (b) high frequency band for the slot monopole at one edge (ME) and (i) the PIFA at the opposite edge (PE) (ii) the PIFA at the center (PC) and (iii) the rotated PIFA at the center (RPC).

ACKNOWLEDGMENT

The authors are thankful to Prof. Jørgen B. Andersen of Aalborg University and Prof. Anders Karlsson of Lund University for helpful discussions.

REFERENCES

[1] M. A. Jensen and J. W. Wallace, "A review of antennas and propagation for MIMO wireless communications," *IEEE Trans. Antennas Propagat.*, vol. 52, no. 11, pp. 2810-2824, Nov. 2004.

[2] B. K. Lau, "Multiple antenna terminals," in *MIMO: From Theory to Implementation*, C. Oestges, A. Sibille, and A. Zanella, Eds. San Diego: Academic Press, 2011, pp. 267-298.

[3] G. J. Foschini and M. J. Gans, "On limits of wireless communications in a fading environment when using multiple antennas," *Wireless Personal Commun.*, vol. 6, pp. 311-335, Mar. 1998.

[4] Z. Ying and D. Zhang, "Study of the mutual coupling, correlations and efficiency of two PIFA antennas on a small ground plane," in *Proc. IEEE Antennas Propagat. Soc. Int. Symp.*, Washington DC, Jul. 2005, pp. 305-308.

[5] B. K. Lau, J. B. Andersen, G. Kristensson, and A. F. Molisch, "Impact of matching network on bandwidth of compact antenna arrays," *IEEE Trans. Antennas Propagat.*, vol. 54, no. 11, pp. 3225-3238, Nov. 2006.

[6] A. Diallo, C. Luxey, P. L. Thuc, R. Staraj, and G. Kossiavas, "Enhanced two-antenna structures for universal mobile telecommunications system diversity terminals," *IET Microw. Antennas Propogat.*, vol. 2, no. 1, pp. 93-101, 2008.

[7] H. Li, J. Xiong, and S. He, "A compact planar MIMO antenna system of four Elements with similar radiation characteristics and isolation structure," *IEEE Antennas Wireless Propagat. Lett.*, vol. 8, pp. 1107-1110, 2009.

[8] Y. Gao, X. Chen, Z. Ying, and C. Parini, "Design and performance investigation of a dual-element PIFA array at 2.5GHz for MIMO terminal," *IEEE Trans. Antennas Propagat.*, vol. 55, no. 12, pp. 3433-3441, Dec. 2007.

[9] B. K. Lau and J. B. Andersen, "Simple and efficient decoupling of compact arrays with parasitic scatterers," *IEEE Trans. Antennas Propagat.*, in press.

[10] S. Dossche, S. Blanch, and J. Romeu, "Optimum antenna matching to minimize signal correlation on a two-port antenna diversity system," *Elect. Lett.*, vol. 40, no. 19, pp. 1164-1165, Sep. 2004.

[11] K. Solbach and C. T. Famdie, "Mutual coupling and chassis-mode coupling small phases array on a small ground plane," in *Proc. Europ. Conf. Antennas Propagat. (EuCAP)*, Edinburgh, UK, Nov. 11-16, 2007.

[12] V. Plicanic, B. K. Lau, A. Derneryd, and Z. Ying, "Actual diversity performance of a multiband diversity antenna with hand and head effects," *IEEE Trans. Antennas Propagat.*, vol. 57, no. 5, pp. 1547-1556, May. 2009.

[13] J. Villanen, J. Ollikainen, O. Kivekas, and P. Vainikainen, "Coupling element based mobile terminal antenna structure," *IEEE Trans. Antennas Propagat.*, vol. 54, no. 7, pp. 2142-2153, Jul. 2006.

[14] T. Taga and K. Tsunekawa, "Performance analysis of a built-in planar inverted-F antenna for 800 MHz band portable radio units," *IEEE J. Select. Areas Commun.*, vol. ACE-5, no. 5, pp.921-929, 1987.

[15] W. L. Schroeder, A. A. Vila, and C. Thome, "Extremely small wideband mobile phone antenna by inductive chassis mode coupling," in *Proc. 36th Europ. Microw. Conf.*, Manchester, UK, Sep. 10-15, 2006, pp. 1702-1705.

[16] W. L. Schroeder and C. T. Famdie, "Utilisation and tuning of the chassis modes of a handheld terminal for the design of multiband radiation characteristics," in *Proc. IEE Wideband Multiband Antennas and Arrays*, Sep. 7, 2005, pp.117-122.

[17] S. R. Best, "The significance of ground-plane size and antenna location in establishing the performance of ground-plane-dependent antennas," *IEEE Antennas Propagat. Mag.* vol. 51, no. 6, pp. 29-42, Dec. 2009.

[18] C. Luxey and D. Manteuffel, "Highly-efficient multiple antenna –system for small MIMO devices," in *Proc. Int. Workshop Antenna Technol. (IWAT)*, Lisbon, Portugal, Mar. 1-3, 2010.

[19] R. F. Harrington and J. R. Mautz, "Theory of characteristic modes for conducting bodies," *IEEE Trans. Antennas Propagat.*, AP-19, no.5, pp. 622-628, Sep. 1971.

[20] P. Vainikainen, J. Ollikainen, O. Kivekas, and I. Kelander, "Resonator-based analysis of the combination of mobile handset antenna and chassis," *IEEE Trans. Antennas Propagat.*, vol. 50, no. 10, pp. 1433-1444, Oct. 2002.

[21] U. Bulus, C. T. Famdie, and K. Solbach, "Equivalent circuit modeling of chassis radiator," in *Proc. German Microw. Conf. (GeMIC2009)*, Munich, Germany, Mar. 16-18, 2009.

[22] C. T. Famie, W. L. Schroeder, and K. Solbach, "Numerical analysis characteristic modes on the chassis of mobile phones," in *Proc. Europ. Conf. Antennas Propagat. (EuCAP)*, France, Nov. 6-10, 2006.

[23] M. C. Fabres, E. A. Daviu, A. V. Nogueiram, and M. F. Bataller, "The theory of characteristic modes revisited: a contribution to the design of antennas for modern applications," *IEEE Trans. Antennas Propagat. Mag.*, vol. 49, no. 5, pp. 52-68, Oct. 2007.

[24] R. J. Garbacz, "A generalized expansion for radiated and scattered field," *IEEE Trans. Antennas Propagat.*, AP-19, pp. 662-668, May 1971.

[25] R. F. Harrington and J. R. Mautz, "Computation of Characteristic modes for conducting bodies," *IEEE Trans. Antennas Propagat.*, AP-19, no. 5, pp. 629-639, Sep. 1971.

[26] S. N. Makarov, *Antenna and EM modeling with MATLAB*, Willey-interscience, 2002.

[27] C. I. Lin and K. L. Wong, "Printed monopole slot antenna for internal multiband mobile phone antenna," *IEEE Trans. Antennas Propagat.*, vol. 55, no. 12, pp. 3690-3697, Dec. 2007.